# Distributed Interval Estimation Methods for Multiagent Systems

Jun Huang, *Member, IEEE*, Haoran Zhang, and Tarek Raïssi, *Senior Member, IEEE*

***Abstract*—This article focuses on the study of distributed interval estimation for networked multiagent systems. For a multiagent system, it has many agents that could build an interconnection topology. For a distributed interval observer, it has many subobservers designed for the corresponding agents. Each subobserver contains two kinds of observer gains: one is determined based on the traditional observer design method and the other one is designed by using the information from the neighborhood. To construct distributed interval observers, two methods are proposed in this article. The first method combines the $H_\infty$ technique with reachability analysis. This method reduces the constraint of design conditions and improves the accuracy of the estimation. However, it needs additional computation. The second one employs the monotone system theory and has no requirement on computation. Finally, two examples are used to compare the two methods.**

***Index Terms*—$H_\infty$ technique, distributed interval observer, monotone system theory, networked multiagents systems, reachability analysis.**

## I. Introduction

Human society is a huge network, and every person is a node in this network. His exchange of information with others strengthens the network. One communicates with new people, and there will be an extra thread between nodes. When he disconnects from someone he once knew, a thread which was originally connected will break. Among them, the idea of graph theory goes back to the fact that researchers had developed autonomous systems of multiple individuals from social animals [1], [2], [3]. Breder [1] had early started to study the mathematical model of shoal aggregation behavior based on the simple local interaction between individuals in the shoal to achieve the coordinated behavior. Besides, the cohesiveness analysis of synchronous and asynchronous swarms with a fixed communication topology was studied in [2] and [3]. In addition to taking inspiration from animal behaviors, researchers also summarized complex networks theoretically. Strogatz [4] focused on the study on unravelling the structure and dynamics of complex networks. Then, researchers found that each agent in a communication topology tends to gather together or moves in the same direction despite the absence of centralized coordination [5], [6].

Nowadays, distributed observer design methods for multiagent systems (MASs) have been widely studied since it has broad applications in power network monitoring [7], output regulation [8], fault diagnosis [9], and so on. In a network topology, since the state of an individual can affect other individuals of its neighborhood through coupling behavior, the observability, or detectability results, which hold for the centralized systems will not be satisfied in MASs. Thus, classical observer design methods are not applicable to MASs either. To study the problem, a leader-following MAS was considered in [10] and distributed observers were used to recover the velocity of the agents. Consensus control could be ensured by a proper protocol in a switched topology. Researchers were devoted to a framework for cooperative tracking control. Both the state and output feedback laws were considered and Luenberger observers were designed to complete the controller design [11]. In the light of the duality in the control theory, a distributed observation problem on linear time-invariant (LTI) systems has been further studied in [12], [13], [14] herein. Mitra and Sundaram designed a kind of distributed observers for LTI MASs [12]. For the mentioned two conditions in the work [12], two different auxiliary matrices were used to transform the shapes of system matrices so as to design distributed observers. Different from the work in [12], a coupling gain was considered and the convergence rate was designed in [13]. After that, a constraint was considered for the coupling gain compared with the previous work [14]. In recent years, distributed observer-based coordination control of MASs has also attracted much attention, such as [15] and [16]. Both full-order observer and reduced-order observer were proposed to complete the consensus protocols in [15]. The single agent in MASs was separated for each one, and a novel observer frame for this problem was proposed in [16]. Besides, there were some important works in the distributed observer design for nonlinear systems [17], [18], [19], [20].

Distributed observers mentioned above are actually asymptotic observers, which recover the system state asymptotically by reconstructing the original system under the help of output values. Nevertheless, these observers are unable to deal with the

Manuscript received 8 December 2021; revised 19 August 2022; accepted 29 November 2022. Date of publication 16 December 2022; date of current version 8 June 2023. This work was supported in part by the Natural Science Foundation of Jiangsu province of China under Grant BK2021-1309 in part by the Open Fund for Jiangsu Key Laboratory of Advanced Manufacturing Technology under Grant HGAMTL-2101, and in part by the open project (Scip202207) of Key Laboratory of System Control and Information Processing, Ministry of Education, China. *(Corresponding author: Jun Huang.)*

Jun Huang is with the School of Mechanical and Electrical Engineering, Soochow University, Suzhou 215131, China, and also with the Key Laboratory of System Control and Information Processing, Ministry of Education, Shanghai 200240, China (e-mail: cauchyhot@163.com).

Haoran Zhang is with the School of Mechanical and Electrical Engineering, Soochow University, Suzhou 215131, China (e-mail: zhrsudaedu@163.com).

Tarek Raïssi is with the Conservatoire National des Arts et Métiers (CNAM), 75141 Paris, France (e-mail: tarek.raissi@cnam.fr).

Digital Object Identifier 10.1109/JSYST.2022.3227051

problems influenced by uncertainty. Then, interval observers have achieved great progress, which were applied in some specific systems, such as LTI systems, nonlinear systems, linear parameter-varying systems, switched systems [21], [22], [23], [24], [25]. These works mainly focused on traditional design methods and the estimation accuracy may not be enough. Meanwhile, the set-membership estimation method was proposed and it was applied to various systems as well [26], [27], [28], [29], [30]. However, both the two methods above were mainly applied in the centralized systems and had some limitations for MASs. To this end, distributed interval observers have been introduced. Recently, the investigation on this topic has been carried out due to its importance in the fields, such as fault detection and isolation [31], coordination control [32], attack detection [33], and so on. A distributed interval observer was designed for detecting and isolating the faults in MASs [31]. Compared with the traditional observer design scheme, the method proposed in [31] used different observer gains for the upper and lower bounds, which caused additional conservation. Controllers based on distributed interval observers were constructed and the coordinate transformation-based method was used in [32]. To avoid the risks in energy-cyber-physical systems, a distributed interval observer was designed to address the fault detection and isolation problem against the bias injection attack in smart energy grid [33]. In order to improve the estimation accuracy, interval residuals were considered and a novel distributed interval observer was introduced [34]. A distributed interval observer was introduced in MASs with time-delays [35]. Besides, the coordinate transformation or orthogonal transformation was usually applied in the distributed interval observer design, which added the additional conservation and increased the difficulty of observer design. However, the interval width from these methods is very large, which is not enough to meet the observation requirements in practical systems.

To solve the problems mentioned above, two distributed interval observer design methods are proposed in this article. One combines the robust observer with reachability analysis technique. And the other one is based on the monotone system theory. For the method based on reachability analysis technique, which is also called interval hull-based method, it uses the set-membership estimation method to design an interval hull for the $H_\infty$ observer, where the interval hull is able to enclose system error. This method first designs a robust observer for MASs suffered from disturbance. Then, the reachability analysis technique employs reachable sets to describe the system state and the disturbance effectively. The interval observer we design based on the monotone system theory requires that the matrix of the error system is positive. On this basis, the error system needs to converge to zero or a bounded constant. To reduce the constraints of system matrices, additional observer gains were designed to guarantee that the error dynamics was positive [31]. Due to the introduction of Laplacian matrix, the information from the neighborhood would have much influence on the system state. By doing this, additional observer gains are necessary for the requirement of positive system and boundness.

There were many previous works about interval observer design methods. In contrast to the observer frame in [25], the second method in our work improves the optimal interval observer design approach in MASs and coordinate transformation could also be added referring to [36]. Different from the recent work in [27] and [37], the first method in this article expands the set-membership based method in MASs. In addition to interval observers, filters are also a useful approach when we need to recover the state. In [38], the optimal filtering performance was obtained based on the matrix decomposition and the fixed-point iterative update rules. Unlike the methods we proposed, the filter only approximates the original state instead of the estimation interval. When the system suffers from a large output noise, the filter would lose efficacy. On the basis of the approaches mentioned above, there were some good surveys summarizing them [39], [40], [41]. Many interval observer design methods were used to deal with the uncertain dynamics systems in [39] and [40]. Meanwhile, the fault detection problem of networked dynamical systems was concerned in [41]. However, these surveys did not focus on distributed interval observer design methods. The traditional interval observer design methods for general systems have many differences when they are applied in distributed systems. To make up for the previous work, we are devoted to the distributed interval observer design of MASs. The main contributions are as follows.

1) Different from the existing works about the interval estimation method for MASs, we focus on the distributed interval observer design in which both traditional centralization observer gains and distributed observer gains are used in the distributed interval observer.
2) For the monotone system theory-based method, we introduce new interval observer gains $\overline{H}$ and $\underline{H}$ to relax the requirement for original systems, which increases the universality of the method.
3) To reduce the requirement on cooperativity of the error system, the reachability analysis technique is applied in the distributed interval observer design, which also further improves the estimation accuracy of the observer.

The rest of this article is organized as follows. Section II gives the necessary preliminaries, including graph theory and system description. Section III presents the interval hull-based method. This section has two subsections, which mainly design a robust observer and construct a reachable set. Section IV provides the distributed interval observer design method based on the monotone system theory. In Section V, a practical example and a numerical example are used to demonstrate that the two methods are both effective. In order to verify the general applicability of two methods, two examples use a directed topology and an undirected topology, respectively. Besides, some comparative results are also discussed in this section. Finally, Section VI concludes this article.

*Notation*: For a matrix $H$, $H^+$ denotes $\max\{0, H\}$, $H^- = H^+ - H$, and $|H| = H^- + H^+$. For a real symmetric matrix $M \in R^{n\times n}$, $M \succ 0 (M \prec 0)$ indicates that $M$ is positive (negative) definite. $\overline{1, N}$ means the set $\{1, \ldots, N\}$. $H^m = [-1, 1]^m$ denotes an interval vector and its each element belongs to $[-1, 1]$. For a discrete transfer function $e(k)$, $\|e(k)\|_2$ denotes its quadratic norm. $I$ is a unit matrix with suitable dimensions.

## II. Problem Formulation and Preliminaries

### A. Introduction to Graph Theory

A digraph $\mathcal{G}(\zeta, \xi, \mathcal{A})$ is considered as a communication topology where $\zeta \in \{1, \ldots, N\}$ means a set of nodes, $\xi \subset \zeta \times \zeta$ is an edge set of ordered pairs of nodes and $\mathcal{A} \in R^{N\times N}$ is an adjacent matrix, which represents the weight between nodes. For $\mathcal{A} = [a_{ij}] \in R^{N\times N}$, $a_{ji}$ is the weight associated with the edge $(i,j) \in \xi$ from node $i$ to node $j$. In this article, the digraph has no self loops, i.e., $a_{ii} = 0, i \in \zeta$. $a_{ji} \neq 0$ if and only if $(i,j) \in \xi$. For node $i$, its neighborhood is denoted as $\zeta_i = \{j | j \in \zeta, a_{ji} \neq 0, j \neq i\}$. A path from $i$ to $j$ means a sequence of successive edges in a form, such as $\{(n_i, n_{i+1}), (n_{i+1}, n_{i+2}), \ldots, (n_{i+k}, n_j)\}$. If $\mathcal{A} = [a_{ij}]$ is the weighted adjacency matrix of graph $\mathcal{G}$, the Laplacian matrix $\mathcal{L}$ of it is defined as $\mathcal{L} := \mathcal{D} - \mathcal{A}$. $\mathcal{D}$ is a diagonal matrix and its $i$th diagonal element is $d_i = \Sigma_{j=1}^{N} a_{ij}$. By definition, $\mathcal{L}$ has a zero eigenvalue with a corresponding eigenvector $1_N$ such that $\mathcal{L}1_N = 0_N$, and if the graph is strongly connected, all the other eigenvalues lie in the open right-half complex plane. If a directed spanning tree exists in a digraph, one or more nodes are necessary to have a directed path approaching to all the other nodes. If a communication graph is supposed to be strongly connected, it means that for any two agents $a$ and $b$, they have at least one path from $a$ to $b$ and one path from $b$ to $a$, respectively. If a topology is called as a balanced topology, the in-degree for each agent is equal to the out-degree for each agent. The in-degree refers to the number of edges to this node, and the out-degree refers to the number of edges from this node to other nodes.

*Lemma 1 (see [42]):* For a strongly connected graph $\mathcal{G}$. Denote that $r = [r_1, \ldots, r_N]^T$ with $r_i > 0, i \in \overline{1, N}$. Assume that the left eigenvector of $\mathcal{L}$ is $r^T$, which is associated with the eigenvalue 0, and $r^T 1_N = 1$. Then $R\mathcal{L} + \mathcal{L}^T R > 0$, where $R = \text{diag}\{r_1, \ldots, r_N\}$.

*Lemma 2 (see [43]):* Following Lemma 1, denote the generalized algebraic connectivity of the digraph $\mathcal{G}$ by $a(\mathcal{L}) = \min_{r^T x = 0, x \neq 0} \frac{x^T (R\mathcal{L} + \mathcal{L}^T R) x}{2x^T R x} > 0$. Moreover, if $\mathcal{G}$ is a balanced graph, $a(\mathcal{L}) = \lambda_2\left(\frac{\mathcal{L}+\mathcal{L}^T}{2}\right)$, where $\lambda_2(A)$ represents the smallest nonzero eigenvalue of $A$.

### B. System Description

For an MAS, consider the single agent as follows:

$$
\begin{aligned}
x_i(k+1) &= Ax_i(k) + \omega_i(k) \\
y_i(k) &= Cx_i(k) + \nu_i(k)
\end{aligned} \tag{1}
$$

where $x_i \in R^n$ is the state of the $i$th agent, $y_i \in R^q$ is the measurable output, $\omega_i(k) \in R^n$ is the unknown disturbance with the lower and upper bounds $\underline{\omega}_i(k) \in R^n$ and $\overline{\omega}_i(k) \in R^n$, and $\nu_i(k) \in R^q$ is the output noise with the lower and upper bounds $\underline{\nu}_i(k)$ and $\overline{\nu}_i(k)$. $A \in R^{n\times n}$ and $C \in R^{q\times n}$ are determined matrices. In what follows, the communication graph is supposed to be strongly connected. The dynamics of the global system is given by

$$
\begin{aligned}
x(k+1) &= \tilde{A}x(k) + \omega(k) \\
y(k) &= \tilde{C}x(k) + \nu(k)
\end{aligned} \tag{2}
$$

where $x = [x_1^T, \ldots, x_N^T]^T$, $\omega = [\omega_1^T, \ldots, \omega_N^T]^T$, $\nu = [\nu_1^T, \ldots, \nu_N^T]^T$, $\tilde{A} = \text{diag}\{\underbrace{A, \ldots, A}_{N}\}$, and $\tilde{C} = \text{diag}\{\underbrace{C, \ldots, C}_{N}\}$.

Due to the fact that the single agent could receive the information from its neighborhood, the dynamics of the observer for $i$th agent is

$$
\begin{aligned}
\hat{x}_i(k+1) = {} & A\hat{x}_i(k) + L_i(y_i(k) - C\hat{x}_i(k)) \\
& + \gamma M_i \sum_{j=1}^{N} a_{ij}(\hat{x}_j - \hat{x}_i)
\end{aligned} \tag{3}
$$

where $i \in \overline{1, N}$, $L_i$ and $M_i$ are the observer gains of the $i$th agent and $\gamma$ is a coupling gain to be designed.

For the agent $i$, denote the error dynamics as

$$
e_i(k) := x_i(k) - \hat{x}_i(k). \tag{4}
$$

Combining (1) with (3), we have the following error dynamics:

$$
e_i(k+1) = \Lambda_i e_i(k) + \gamma M_i \sum_{j=1}^{N} a_{ij}(\hat{e}_j(k) - \hat{e}_i(k)) + B_i d_i(k) \tag{5}
$$

with $\Lambda_i = A - L_i C$, $B_i = [I \ \ -L_i]$, $d_i(k) = \begin{bmatrix} \omega_i(k) \\ \nu_i(k) \end{bmatrix}$.

Let $e(k) := [e_1^T(k), \ldots, e_N^T(k)]^T$, and the dynamics of the global system error is

$$
e(k+1) = \Lambda e(k) - \gamma \bar{M}(\mathcal{L} \otimes I_n)e(k) + Bd(k) \tag{6}
$$

where

$$
\begin{aligned}
\Lambda &= \text{diag}\{A - L_1 C, \ldots, A - L_N C\} \\
\bar{M} &= \text{diag}\{M_1, \ldots, M_N\} \\
B &= \text{diag}\{B_1, \ldots, B_N\} \\
d(k) &= [d_1^T(k), \ldots, d_N^T(k)]^T.
\end{aligned}
$$

## III. Distributed Interval Observer Design Based on Reachability Analysis

### A. Distributed $H_\infty$ Observer Design

In this part, we design a distributed robust observer and give the sufficient conditions of the observer. The goal is to prove the stability of the observer and the convergence of the system error.

*Definition 1 (see [44]):* An observer has an $H_\infty$ performance if it satisfies the following two conditions.

1) if $d(i) = 0$, the error system is asymptotically stable;
2) if $d(i) \neq 0$, the following inequality holds:

$$
\sum_{i=0}^{\infty} e^T(i)e(i) \leq \phi \sum_{i=0}^{\infty} d^T(i)d(i)
$$

with $\phi > 0$ and $e(0) = 0$.

*Theorem 1:* If there exists a constant $\phi > 0$ and matrices $P \succ 0, L, \bar{M}$ such that

$$\begin{cases} \begin{bmatrix} -P+I & * & * \\ 0 & -\phi I & * \\ P\Omega & PB & -P \end{bmatrix} \prec 0 \\ \gamma > \frac{1}{\alpha(\mathcal{L})} \end{cases} \tag{7}$$

where $\Omega = \Lambda - \gamma\bar{M}(\mathcal{L} \otimes I_n)$, $\bar{M} = P^{-1}$, and $U = PL$, then (3) is a distributed robust observer.

*Proof:* For (7), since the matrix $P$ is positive definite, it is obvious that $-P \prec 0$ and Schur Complement could be used here. Under the transformation and suitable computation, (7) is equal to

$$\begin{bmatrix} \Omega^T P\Omega - P + I & \Omega^T PB \\ B^T P\Omega & B^T PB - \phi I \end{bmatrix} \prec 0. \tag{8}$$

The considered system is subject to disturbances and output noises, the part 2 of Definition 1 is used to prove Theorem 1.

Denote

$$H = \sum_{k=0}^{\infty} e^T e - \phi \sum_{k=0}^{\infty} d^T d. \tag{9}$$

Construct a Lyapunov function as

$$V = e^T Pe. \tag{10}$$

Then, the increment of (10) is

$$\triangle V(k) = V(k+1) - V(k). \tag{11}$$

Considering the initial condition $e(0) = 0$, it follows from (11) that

$$\begin{aligned} \sum_{k=0}^{\infty} \Delta V(k) = & \lim_{k\to\infty} \{V(k) - V(k-1) \\ & + V(k-1) - V(k-2) + \cdots - V(0)\} \\ = & \lim_{k\to\infty} \{V(k) - V(0)\} \\ = & \lim_{k\to\infty} \{V(k)\} \geq 0. \end{aligned}$$

Then, (9) could be rewritten as

$$H \leq \sum_{k=0}^{\infty} \left[e^T e - \phi d^T d + \Delta V\right]. \tag{12}$$

Let $J = e^T e - \phi d^T d + \Delta V$. Substituting (6) into $J$, we have

$$\begin{aligned} J = & e^T(k)e(k) - \phi d^T(k)d(k) \\ & + e^T(k+1)Pe(k+1) - e^T(k)Pe(k) \\ = & e^T e - \phi d^T d - e^T Pe \\ & + (e^T\Omega^T + d^T(k)B^T)P(\Omega e + Bd) \\ = & e^T(\Omega^T P\Omega + I - P)e + d^T(B^T PB - \phi I)d \\ & + e^T\Omega^T PBd + d^T B^T P\Omega e \\ = & \begin{bmatrix} e^T & d^T \end{bmatrix} \begin{bmatrix} \Omega^T P\Omega - P + I & \Omega^T PB \\ B^T P\Omega & B^T PB - \phi I \end{bmatrix} \begin{bmatrix} e \\ d \end{bmatrix}. \end{aligned} \tag{13}$$

According to (8), it follows that

$$J(k) < 0. \tag{14}$$

From (12) and (14), we deduce

$$H \leq \sum_{k=0}^{\infty} J(k) \leq 0. \tag{15}$$

Combining (9) and (15), the condition 2 of Definition 1 is satisfied and (3) is a distributed robust observer.

*Remark 1:* In Theorem 1, the parameter $\gamma$ is corresponding with $\alpha(\mathcal{L})$, which represents the generalized algebraic connectivity of a graph. If a graph is more stable, $\alpha(\mathcal{L})$ tends to be larger. Using this method, $\gamma$ will have more range to be chosen.

### B. Interval Hull Design

*Definition 2 (see [26]):* An $\alpha$-dimensional zonotope $\Im$ is defined as

$$\Im = \sigma \oplus QH^\alpha = \sigma + Q\chi, \chi \in H^\alpha$$

with $\sigma \in R^\iota$, $Q \in R^{\iota\times\alpha}$, and $H^\alpha = [-1, 1]^\alpha$. For simplicity, zonotope $\Im$ is described by $\langle\sigma, Q\rangle$.

*Property 1 (see [27]):* For two zonotopes $\Im_1 = \langle\sigma_1, Q_1\rangle$ and $\Im_2 = \langle\sigma_2, Q_2\rangle$, their Minkowski sum is

$$\Im_1 \oplus \Im_2 = \langle\sigma_1 + \sigma_2, [Q_1\ Q_2]\rangle.$$

For zonotopes $\Im_k \subset R^\iota, k \in \{1, \ldots, r\}$, the Minkowski sum of them is

$$\bigoplus_{k=1}^{r} \Im_k = \Im_1 \oplus \Im_2 \oplus \ldots \oplus \Im_r.$$

*Definition 3 (see [29]):* Considering a $s$-order zonotope $\Im$, there exists an interval hull, which could totally contain $\Im$. The interval hull is considered as the smallest interval vector for the corresponding zonotope

$$\Im \subset \blacksquare(\Im) = [\mu, \nu]$$

where $\mu = [\mu_1, \ldots, \mu_s]^T$, $\nu = [\nu_1, \ldots, \nu_s]^T$ and $\blacksquare$ represents the interval hull.

*Property 2 (see [45]):* If $\Im = \langle\sigma, Q\rangle, \sigma \in R^\iota$ and $Q \in R^{\iota\times\alpha}$, the components of its interval hull is

$$\begin{cases} \mu_i = \sigma_i - \Sigma_{j=0}^{\alpha}|Q_{ij}|, & i = 1, \ldots, \iota \\ \nu_i = \sigma_i + \Sigma_{j=0}^{\alpha}|Q_{ij}|, & i = 1, \ldots, \iota. \end{cases} \tag{16}$$

*Property 3 (see [45]):* Given zonotopes $\Im_i, i \in \{1, \ldots, m\}$

$$\blacksquare\left(\bigoplus_{k=1}^{m} \Im_k\right) = \bigoplus_{k=1}^{m} (\blacksquare\Im_k).$$

*Assumption 1:* $d(k), x_0$, and $e(0)$, which represents the disturbance, initial state, and initial error, could be wrapped as follows:

$$\begin{aligned} d(k) &\in \Im_d = \langle 0, D_d\rangle \\ x(0) &\in \Im_{x_0} = \langle\sigma_0, Q_0\rangle \\ e(0) &\in \Im_{e_0} = \langle 0, Q_0\rangle \end{aligned} \tag{17}$$

where $Q_0$ is given matrix and $D_d = \mathrm{diag}\{\overline{d}_i\}$.

Based on the robust observer (3), an interval observer based on reachability analysis technique is designed as

$$\begin{cases}\overline{x} = \hat{x} + \overline{e} \\ \underline{x} = \hat{x} + \underline{e}\end{cases} \tag{18}$$

where $\overline{e}$ and $\underline{e}$ are introduced in Theorem 2.

*Theorem 2:* Based on Assumption 1, an interval estimation of the system state given by (18) and the bounds of the error $e(k)$ are given

$$[\underline{e}(k), \overline{e}(k)] = \Omega^k \blacksquare(\Im_{e_0}) \oplus \bigoplus_{i=0}^{k-1} \Omega^{k-i-1} B \blacksquare(\Im_d) \tag{19}$$

*Proof:* For the error system (6), by iteration we have

$$e(k) = \Omega^k e(0) + \sum_{i=0}^{k-1} \Omega^{k-i-1} B d(i). \tag{20}$$

Denote $\Im_k$ as the zonotope of $e(k)$. Substitute Assumption 1 into (20)

$$\Im_k = \Omega^k \Im_{e_0} \oplus \bigoplus_{i=0}^{k-1} \Omega^{k-i-1} B \Im_d. \tag{21}$$

According to Definition 3, the interval hull of $e(k)$ could be derived as

$$\begin{aligned}[\underline{x}(k), \overline{x}(k)] &= \blacksquare\left(\Omega^k \Im_{e_0}\right) \oplus \blacksquare\left(\bigoplus_{i=0}^{k-1} \Omega^{k-i-1} B \Im_d\right) \\ &= \Omega^k \blacksquare(\Im_{e_0}) \oplus \bigoplus_{i=0}^{k-1} \Omega^{k-i-1} B \blacksquare(\Im_d). \end{aligned} \tag{22}$$

*Remark 2:* Theorem 1 gives sufficient conditions of robust observers, which implies that the observer is immune to the external interference and the output noise. Under the result of Theorem 1, we can ensure that there exists a bounded interval hull that could enclose the error and disturbance. After that, Theorem 2 deduces the interval hull of $e(k)$ from the known interval hull of $e(0)$. By combining Theorem 1 with Theorem 2, the interval hull-based method is proposed.

## IV. Distributed Interval Observer Based on the Monotone System Theory

In this section, an interval observer design method for MASs based on the monotone system theory is proposed.

*Lemma 3:* Given a real matrix $T \in R^{m\times n}$ and a vector $\alpha \in n \times 1$, if there exists $\underline{\alpha}$ and $\overline{\alpha}$ such that $\alpha \in [\underline{\alpha}, \overline{\alpha}]$, then

$$T^+\underline{\alpha} - T^-\overline{\alpha} \leq T\alpha \leq T^+\overline{\alpha} - T^-\underline{\alpha}.$$

To satisfy the requirement $\underline{x} \leq x \leq \overline{x}$, the following observer for agent $i$ is considered:

$$\begin{aligned}\overline{x}_i(k+1) &= (A - L_iC)\overline{x}_i(k) + L_iy(k) + \overline{H}_i(\overline{x}_i(k) - \underline{x}_i(k)) \\ &\quad + \gamma M_i \sum_{j=1}^{N} a_{ij}(\overline{x}_j - \overline{x}_i) + B^+\overline{d}_i(k) - B^-\underline{d}_i(k) \\ \underline{x}_i(k+1) &= (A - L_iC)\underline{x}_i(k) + L_iy(k) - \underline{H}_i(\overline{x}_i(k) - \underline{x}_i(k)) \\ &\quad + \gamma M_i \sum_{j=1}^{N} a_{ij}(\underline{x}_j - \underline{x}_i) + B^+\underline{d}_i(k) - B^-\overline{d}_i(k). \end{aligned} \tag{23}$$

Then, the dynamics of the global observer system is given by

$$\begin{cases}\overline{x}(k+1) = \Omega\overline{x}(k) + Ly(k) + \overline{H}(\overline{x}(k) - \underline{x}(k)) \\ \qquad\qquad +B^+\overline{d}(k) - B^-\underline{d}(k) \\ \underline{x}(k+1) = \Omega\underline{x}(k) + Ly(k) - \underline{H}(\overline{x}(k) - \underline{x}(k)) \\ \qquad\qquad +B^+\underline{d}(k) - B^-\overline{d}(k)\end{cases} \tag{24}$$

with

$$\underline{d} = \begin{bmatrix}\underline{d}_1 \\ \vdots \\ \underline{d}_N\end{bmatrix}, \underline{H} = \begin{bmatrix}\underline{H}_1 & & \\ & \ddots & \\ & & \underline{H}_N\end{bmatrix}$$
$$\overline{d} = \begin{bmatrix}\overline{d}_1 \\ \vdots \\ \overline{d}_N\end{bmatrix}, \overline{H} = \begin{bmatrix}\overline{H}_1 & & \\ & \ddots & \\ & & \overline{H}_N\end{bmatrix}.$$

For traditional interval observers, the following assumptions are necessary.

*Assumption 2:* For the uncertain disturbance $\omega$ and the output noise $\nu$, we have

$$-\overline{\omega} = \underline{\omega} \leq \omega \leq \overline{\omega}$$
$$-\overline{\nu} = \underline{\nu} \leq \nu \leq \overline{\nu}$$
$$-\overline{d} = \underline{d} \leq d \leq \overline{d}.$$

*Assumption 3:* There exist observer gains $L$, $H$, and $\bar{M}$ such that $\Psi$ is nonnegative, for all $i \in \overline{1, N}$, with

$$\Psi = \begin{bmatrix}\Omega + \overline{H} & \overline{H} \\ \underline{H} & \Omega + \underline{H}\end{bmatrix}.$$

*Assumption 4:* For the initial system state, we have

$$\underline{x}_0 \leq x_0 \leq \overline{x}_0.$$

*Theorem 3:* If Assumptions 2–4 are satisfied, the bounds $\underline{x}$ and $\overline{x}$ given by (24) satisfy $\underline{x} \leq x \leq \overline{x}$.

*Proof:* Define the boundary of the estimation error as

$$\begin{cases}\overline{\epsilon}(k+1) = \overline{x}(k+1) - x(k+1) \\ \qquad\qquad = \Omega\overline{\epsilon}(k) + \underline{H}(\overline{\epsilon}(k) + \underline{\epsilon}(k)) + \overline{\xi}(k) \\ \underline{\epsilon}(k+1) = x(k+1) - \underline{x}(k+1) \\ \qquad\qquad = \Omega\underline{\epsilon}(k) + \underline{H}(\overline{\epsilon}(k) + \underline{\epsilon}(k)) + \underline{\xi}(k)\end{cases} \tag{25}$$

i.e.,

$$\begin{bmatrix}\overline{\epsilon}(k+1) \\ \underline{\epsilon}(k+1)\end{bmatrix} = \Psi \begin{bmatrix}\overline{\epsilon}(k) \\ \underline{\epsilon}(k)\end{bmatrix} + \begin{bmatrix}\overline{\xi}(k) \\ \underline{\xi}(k)\end{bmatrix} \tag{26}$$

with

$$\overline{\xi}(k) = (B^+\overline{d}(k) - B^-\underline{d}(k)) - Bd(k)$$
$$\underline{\xi}(k) = Bd(k) - (B^+\underline{d}(k) - B^-\overline{d}(k)).$$

To prove the validity of (23) and (24), it is necessary to prove the nonnegativeness of the error system. From Assumption 2 and Lemma 3, one can deduce that $\overline{\xi}(k) \geq 0$ and $\underline{\xi}(k) \geq 0$. From Assumption 4, it is obvious that $\overline{\epsilon}(0) \geq 0$ and $\underline{\epsilon}(0) \geq 0$ hold. By Assumption 3, we have $\Psi$ is nonnegative. Above all, considering the monotone system theory, $\begin{bmatrix}\overline{\epsilon}(k)\\ \underline{\epsilon}(k)\end{bmatrix} > 0$ holds, which is equivalent to $\underline{x} \leq x \leq \overline{x}$ for all $k \in Z^{+}$. Hence, Theorem 3 could be proven.

After the proof of boundedness, we mainly focus on the design of observer gains $L$, $\underline{H}$, $\overline{H}$, and $\bar{M}$ to ensure the stability of observer (24). Besides, the gains also have much influence on the accuracy of the interval estimation. Thus, in addition to consider the ultimate-bound problem, the interval width of the proposed observer is also an important factor. In this way, how to minimize the following cost function would be a feasible problem here:

$$\begin{aligned} &\underset{L,\bar{M},\underline{H},\overline{H}}{\text{minimize}} && \tau^2 \\ &\text{subject to} && \frac{\|\epsilon\|_2^2}{\|\xi\|_2^2} \leq \tau^2. \end{aligned} \tag{27}$$

In (27), $\epsilon = \overline{x} - \underline{x}$, while $\xi = \overline{d}$ is corresponding with the bound of the disturbance $\omega(k)$ and the output noise $\nu(k)$. From this cost function, we can obtain the optimal observer gains by finding suitable observer gains such that $\tau$ is the minimum. Through searching for the smallest $\tau$, the error $\epsilon$ has been scaled down considering the constant value $\overline{d}(k)$. According to the definition of $\epsilon$, it follows that

$$\epsilon(k+1) = (\Lambda - \gamma\bar{M}(\mathcal{L} \otimes I_n) + \underline{H} + \overline{H})\epsilon(k) + 2|B|\overline{d}(k). \tag{28}$$

Then, the bounded-real lemma has been used to transform (27) into the following inequality:

$$\epsilon^T(k+1)F\epsilon(k+1) - \epsilon^T(k)F\epsilon(k) \leq -\epsilon^T(k)\epsilon(k) + \tau^2\xi^T(k)\xi(k) \tag{29}$$

where $F \in R^{nN\times nN} \succ 0$ is a symmetric matrix.

*Theorem 4:* Under the conditions of Theorem 3, if there exists a matrix $F$ such that

$$\begin{bmatrix} -F+I & * & * \\ 0 & -\tau^2 I & * \\ F\Omega + F\overline{H} + F\underline{H} & 2F|B| & -F \end{bmatrix} \preceq 0 \tag{30}$$

then the observer gains $L$, $\underline{H}$, $\overline{H}$, and $\bar{M}$ are optimal observer gains.

*Proof:* To be more concrete, inequality (30) could be converted to with (31), shown at the bottom of this page.

$$\begin{aligned} \Pi_{ii} &= P_iA_i - Q_iC_i + P_i\overline{H}_i + P_i\underline{H}_i - \gamma d_iP_iM_i \\ \Pi_{ij} &= \gamma a_{ij}P_iM_i \\ F_i|B_i| &= [F_i,\ |Q_i|] \\ |Q_i| &= F_i|L_i| \\ Q_i &= F_iL_i. \end{aligned}$$

Substituting (28) into (29), one can obtain that

$$\begin{aligned} &((\Omega + \underline{H} + \overline{H})\epsilon + 2|B|d)^T F((\Omega + \underline{H} + \overline{H})\epsilon + 2|B|d) \\ &\quad - \epsilon^T F\epsilon \leq -\epsilon^T\epsilon + \tau^2 d^T d \end{aligned} \tag{32}$$

i.e.,

$$\begin{bmatrix} \Xi^T F\Xi - F + I & * \\ 2|B|^T F\Xi & 4|B|^T F|B| - \tau^2 I \end{bmatrix} \preceq 0 \tag{33}$$

with $\Xi = \Omega + \underline{H} + \overline{H}$, it could be transformed into

$$\begin{bmatrix} -F+I & 0 \\ 0 & -\tau^2 I \end{bmatrix} - \begin{bmatrix} \Xi^T F \\ 2|B|^T F \end{bmatrix} (-F)^{-1} \begin{bmatrix} F\Xi & 2F|B| \end{bmatrix} \preceq 0. \tag{34}$$

By using Schur complements, (34) can be verified that

$$\begin{bmatrix} -F+I & * & * \\ 0 & -\tau^2 I & * \\ F(\Omega + \underline{H} + \overline{H}) & 2F|B| & -F \end{bmatrix} \preceq 0. \tag{35}$$

*Remark 3:* Compared with the algorithm proposed in [31], we add the distributed observer gains $M_i$ in the two proposed methods, which enable each sub observer to communicate with

$$\begin{bmatrix} -F_1+I & \cdots & 0 & * & \cdots & * & * & \cdots & * \\ \vdots & \ddots & \vdots & \vdots & \ddots & \vdots & \vdots & \ddots & \vdots \\ 0 & \cdots & -F_N+I & * & \cdots & * & * & \cdots & * \\ 0 & \cdots & 0 & -\tau^2 I & \cdots & 0 & * & \cdots & * \\ \vdots & \ddots & \vdots & \vdots & \ddots & \vdots & \vdots & \ddots & \vdots \\ 0 & \cdots & 0 & 0 & \ddots & -\tau^2 I & * & \ddots & * \\ \Pi_{11} & \cdots & \Pi_{1N} & 2F_1|B_1| & \cdots & 0 & -F_1 & \cdots & 0 \\ \vdots & \ddots & \vdots & \vdots & \ddots & \vdots & \vdots & \ddots & \vdots \\ \Pi_{N1} & \cdots & \Pi_{NN} & 0 & \ddots & 2F_N|B_N| & 0 & \ddots & -F_N \end{bmatrix} < 0 \tag{31}$$

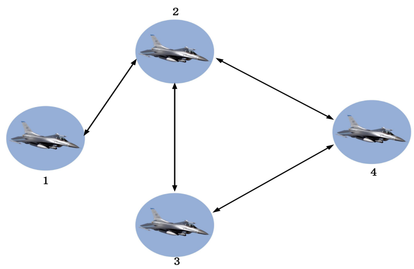


Fig. 1. Communication graph of four F-18 aircrafts.

TABLE I
INITIAL STATES OF EXAMPLE 1

| | value | | value |
|---|---|---|---|
| $\alpha$ of agent 1 | 1 | $\alpha$ of agent 3 | 1 |
| $\overline{\alpha}$ of agent 1 | 3 | $\overline{\alpha}$ of agent 3 | 3 |
| $\underline{\alpha}$ of agent 1 | –1 | $\underline{\alpha}$ of agent 3 | 0 |
| $q$ of agent 1 | 5 | $q$ of agent 3 | 4 |
| $\overline{q}$ of agent 1 | 8 | $\overline{q}$ of agent 3 | 5 |
| $\underline{q}$ of agent 1 | 2 | $\underline{q}$ of agent 3 | 1 |
| $\alpha$ of agent 2 | –3 | $\alpha$ of agent 4 | –2 |
| $\overline{\alpha}$ of agent 2 | –1 | $\overline{\alpha}$ of agent 4 | 1 |
| $\underline{\alpha}$ of agent 2 | –5 | $\underline{\alpha}$ of agent 4 | –4 |
| $q$ of agent 2 | 2 | $q$ of agent 4 | –4 |
| $\overline{q}$ of agent 2 | 3 | $\overline{q}$ of agent 4 | –2 |
| $\underline{q}$ of agent 2 | 1 | $\underline{q}$ of agent 4 | –5 |

each other. Besides, we use only one centralization observer gains $L_i$ while [31] occupied two gains $\overline{L}_i$ and $\underline{L}_i$, which would increase additional computation burden of the algorithm. Different from the algorithm in [46], we use the cost function to reduce the influence of external disturbance on the estimation interval, while researchers in [46] only considered the problem of robustness in consensus control. If distributed interval observer design methods in this article are integrated into the consensus protocol design in [46], it may play a better effect.

## V. SIMULATION

This section contains two examples. The first one is a team of aircraft model with an undirected graph and the other one is a numerical exapmle with a directed graph. Two examples are both running in CPU Inter Core i7-6700HQ CPU of 2.60 GHZ, memory 8 GB. The main software used is MATLAB 2020a with Zonotope Toolboxes.

*Example 1:* Consider an MAS from [31]. The communication topology is shown in Fig. 1, which is an undirected topology. The dynamics of the system is borrowed from [31]. It is a two-dimension system and has states $\alpha_i(k)$ and $q_i(k)$, which mean the angle of attack and the pitch rate of each aircraft, respectively.

Consider (1) with the matrices

$$A = \begin{bmatrix} 0.8825 & 0.0987 \\ -0.8458 & 0.9122 \end{bmatrix}, C = \begin{bmatrix} 1 & 0.2 \end{bmatrix}.$$

The initial states, the external disturbance and the output noise are shown in Tables I and II.

TABLE II
DISTURBANCE AND NOISE OF EXAMPLE 1

| Agent | Disturbance | Noise |
|---|---|---|
| 1 | $0.2 + 0.1\lvert\cos(0.5k)\rvert$ | $0.1\sin(k)$ |
| 2 | $0.1\cos(0.1k)$ | $0.1\sin(k)$ |
| 3 | $\cos(0.2\pi k) + 0.3\sin(0.2\pi k)$ | $0.01\sin(k)$ |
| 4 | $\cos(0.3\pi k) + 0.1\sin(0.3\pi k)$ | $0.05\sin(k)$ |

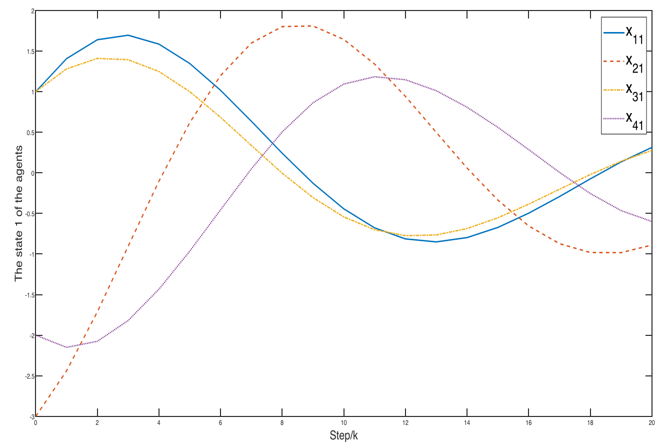


Fig. 2. Bounds of state 1 for four agents.

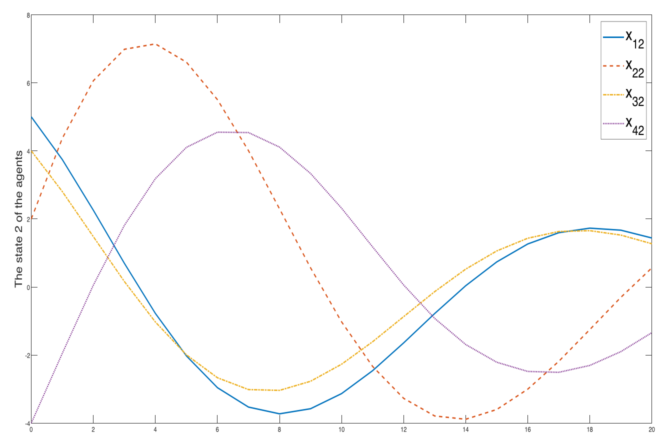


Fig. 3. Bounds of state 2 for four agents.

From Lemmas 1 and 2, we have $\alpha(\mathcal{L}) = 0.5$, then we have $\gamma > 2$. In this section, $\gamma = 3$ is applied. The results are as follows. Figs. 2 and 3 show the state 1 and state 2 of the four agents. In Figs. 4 and 5 , $v_{ij}$ represents the bounds obtained from the monotone system theorem-based method and $u_{ij}$ represents the bounds obtained from interval hull-based method, where $i$ means the $i$th agent and $j$ represents the $j$th state.

*Example 2:* The second example is an MAS with a directed graph, which is to further verify the validity of the two proposed method. The state-space dynamics is

$$\begin{cases} x_i(k+1) = Ax_i(k) + Bu_i(k) + \omega_i(k) \\ y_i(k) = Cx_i(k) + \nu_i(k) \end{cases}$$

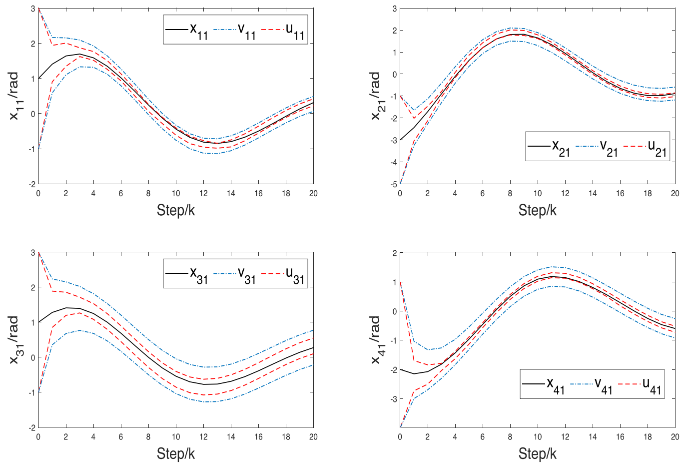


Fig. 4. Bounds of state 1 for four agents.

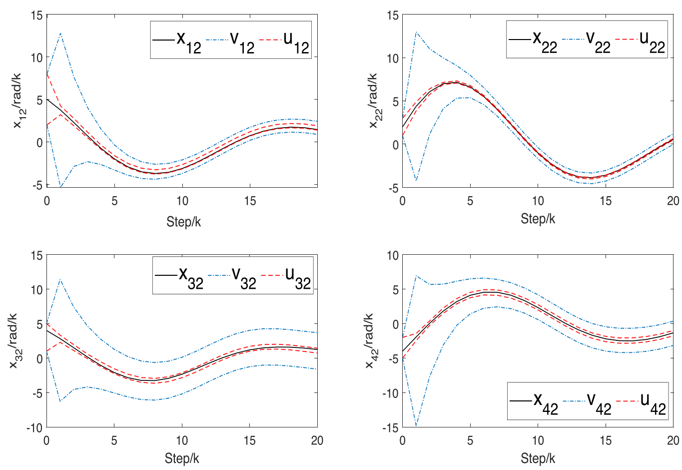


Fig. 5. Bounds of state 2 for four agents.

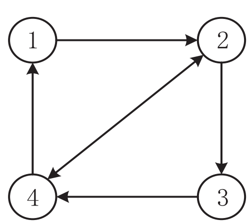


Fig. 6. Communication topology of Example 2.

where

$$A = \begin{bmatrix} 0.2 & 1 \\ 0.1760 & 0.2415 \end{bmatrix}, B = \begin{bmatrix} 1 \\ 1 \end{bmatrix}, C = \begin{bmatrix} 0.8 & 0.2 \end{bmatrix}.$$

The directed topology is shown in Fig. 6 . Then, the matrix $\mathcal{L}$ is as follows:

$$\mathcal{L} = \begin{bmatrix} 1 & -1 & 0 & 0 \\ 0 & 2 & -1 & -1 \\ 0 & 0 & 1 & -1 \\ -1 & -1 & 0 & 2 \end{bmatrix}. \quad (36)$$

The initial states, the external disturbance and the output noise are shown in Tables III and IV. For $i \in \{1, \ldots, N\}$, the input of them are all $u_i(k) = \sin(k)$.

TABLE III
INITIAL STATE OF EXAMPLE 2

| | value | | value |
|---|---|---|---|
| $\alpha$ of agent 1 | 5.5 | $\alpha$ of agent 3 | –3.2 |
| $\overline{\alpha}$ of agent 1 | 7.5 | $\overline{\alpha}$ of agent 3 | –1.2 |
| $\underline{\alpha}$ of agent 1 | 3.5 | $\underline{\alpha}$ of agent 3 | –5.2 |
| $q$ of agent 1 | –2.8 | $q$ of agent 3 | –1.9 |
| $\overline{q}$ of agent 1 | –0.8 | $\overline{q}$ of agent 3 | 0.1 |
| $\underline{q}$ of agent 1 | –4.8 | $\underline{q}$ of agent 3 | –3.9 |
| $\alpha$ of agent 2 | 4.3 | $\alpha$ of agent 4 | 2.4 |
| $\overline{\alpha}$ of agent 2 | 6.3 | $\overline{\alpha}$ of agent 4 | 4.4 |
| $\underline{\alpha}$ of agent 2 | 2.3 | $\underline{\alpha}$ of agent 4 | 0.4 |
| $q$ of agent 2 | –1.6 | $q$ of agent 4 | 1.5 |
| $\overline{q}$ of agent 2 | 0.4 | $\overline{q}$ of agent 4 | 3.5 |
| $\underline{q}$ of agent 2 | –3.6 | $\underline{q}$ of agent 4 | –0.5 |

TABLE IV
DISTURBANCE AND NOISE OF EXAMPLE 2

| Agent | Disturbance | Noise |
|---|---|---|
| 1 | $0.1\sin(0.5k)$ | $0.05\sin(k)$ |
| 2 | $0.1\sin(0.5k)$ | $0.05\sin(k)$ |
| 3 | $0.1\sin(0.5k)$ | $0.05\sin(k)$ |
| 4 | $0.1\sin(0.5k)$ | $0.05\sin(k)$ |

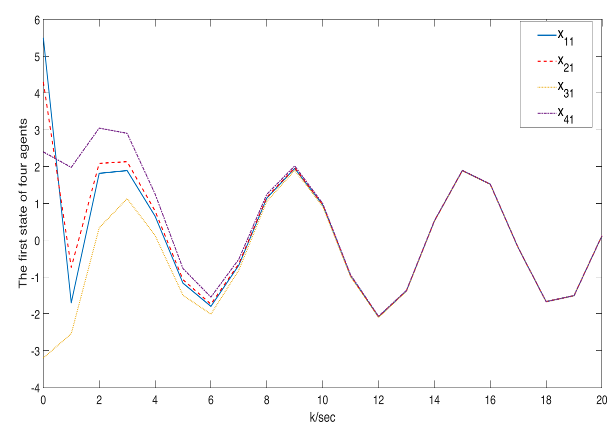


Fig. 7. Bounds of state 1 for four agents.

From Lemmas 1 and 2, we have $a(\mathcal{L}) = 2$, then we have $\gamma > 0.5$. In Example 2, $\gamma$ is chosen as 2. The simulation results are as follows. Figs. 7 and 8 show the state of four agents. In Figs. 9 and 10, $u_{ij}$ represents the bounds obtained from the monotone system theorem-based method and $v_{ij}$ represents the bounds obtained from interval hull-based method, where $i$ means the $i$th agent and $j$ is the $j$th state.

From the results, one can obtain that the state of agents can be included in the bounds from distributed interval observers. By comparison we can see that the width of the interval from the interval hull-based method is tighter than that from the monotone system theory-based method. Besides, from Tables V and VI, it is obvious that the interval hull-based method needs more computation time than the monotone system theory-based method.

*Remark 4:* The monotone system theory is discussed, for example, in [47]. For continuous-time linear systems, a monotone system requires that the system matrix should be Metzler.

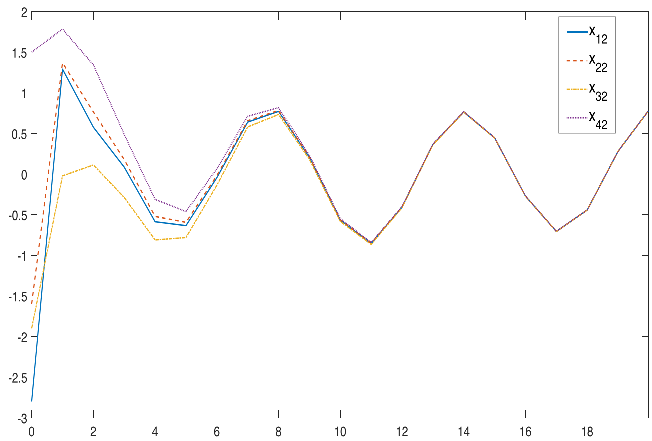


Fig. 8. Bounds of state 2 for four agents.

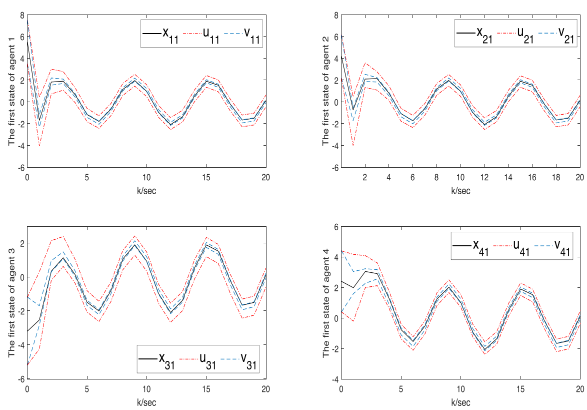


Fig. 9. Bounds of state 1 for four agents.

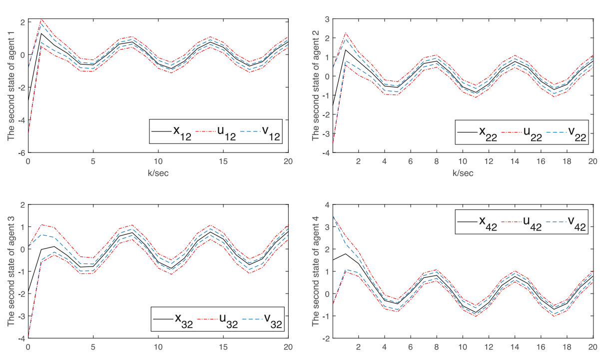


Fig. 10. Bounds of state 2 for four agents.

For discrete-time linear systems, the system matrix conforms to be a nonnegative matrix. The interval hull-based method combines the robust observer with reachability analysis [48]. Both two methods have their own advantages. The interval hull-based method further improves the estimation accuracy of the observer compared with the monotone system theory-based method. Meanwhile, the interval hull-based method does not require the system matrix be a nonnegative matrix, which relaxes the design conditions of the observer compared to the previous work. Moreover, the monotone system theory-based method has less computation burden compared with the interval hull-based method, which is shown in Tables V and VI.

TABLE V
COMPUTATION TIME COMPARISON OF EXAMPLE 1

| | Monotone system theory method | Interval hull-based method |
|---|---|---|
| Gains computation | 0.263 s | 0.295 s |
| Box design | 0 s | 1.482 s |
| Observer design | 0.961 s | 0.583 s |
| The total time | 1.224 s | 2.360 s |

TABLE VI
COMPUTATION TIME COMPARISON OF EXAMPLE 2

| | Monotone system theory-based method | Interval hull-based method |
|---|---|---|
| Gains computation | 0.352 s | 0.283 s |
| Box design | 0 s | 1.772 s |
| Observer design | 0.597 s | 0.627 s |
| The total time | 0.949 s | 2.682 s |

*Remark 5:* A novel distributed interval estimation method was proposed for sensor networks under the denial-of-service attack and the adaptive event-triggered protocol [49]. Although it obtains the boundary of MASs by distributed interval estimation technique, it still differs from the methods in this article in two aspects. First, the objects are different. It is easy to find that the system dynamics in [49] is different from that in our work, which mainly reflects in the output matrix. Sensor networks are the background of [49] and many subobservers are combined to complete the interval estimation of the total plant, and the main idea is to split a high-dimensional output matrix into numerous independent output matrices. However, in our work, the output matrix is a separated matrix for each agent. Second, there are some differences in observer structures. The distributed interval estimator in [49] mainly uses distributed estimator gains to construct estimation intervals. Nevertheless, we consider additional centralization observer gains for distributed interval observer because it may play an important role when we need to obtain the state of each agent.

## VI. CONCLUSION

Two distributed interval observer design methods are presented for MASs subject to uncertainty. Interval estimation plays an important role in fields, which need to recover the boundaries of the system state. In this article, the first proposed method combines the $H_\infty$ technique with reachability analysis. It could achieve a tight interval width and reduces the requirements for system matrices. However, it would have some computation burden compared with the second method. The second proposed method requires error systems to be cooperative systems, which would cause the design constraints. Besides, extra observer gains of the second method would also generate that the boundaries are larger than that of the first method. Finally, two examples are used to prove the effectiveness of our results. By analyzing the simulation results, we find that the interval hull-based method has obvious advantages compared with the second method. State estimation is an important procedure for fault diagnosis and various control aims. So in the future, we may focus on the study of distributed control protocol design for MASs and fault diagnosis.

## References


[1] C. Breder, "Equations descriptive of fish schools and other animal aggregations," *Ecology*, vol. 35, no. 3, pp. 361–370, 1954.

[2] V. Gazi and K. Passino, "Stability analysis of swarms," *IEEE Trans. Autom. Control*, vol. 48, no. 4, pp. 692–697, Apr. 2003.

[3] V. Gazi and K. Passino, "Stability analysis of social foraging swarms," *IEEE Trans. Syst., Man, Cybern.*, vol. 34, no. 1, pp. 539–557, Feb. 2004.

[4] S. Strogatz, "Exploring complex networks," *Nature*, vol. 410, no. 6825, pp. 268–276, 2001.

[5] A. Jadbabaie, J. Lin, and A. Morse, "Coordination of groups of mobile autonomous agents using nearest neighbor rules," *IEEE Trans. Autom. Control*, vol. 48, no. 6, pp. 988–1001, Jun. 2003.

[6] T. Vicsek, A. Czirok, E. Ben-Jacob, I. Cohen, and O. Sochet, "Novel type of phase transition in a system of self-driven particles," *Phys. Rev. Lett.*, vol. 75, no. 6, pp. 1226–1229, 2006.

[7] F. Pasqualetti, R. Carli, and F. Bullo, "Distributed estimation via iterative projections with application to power network monitoring," *Automatica*, vol. 48, no. 5, pp. 747–758, 2012.

[8] H. Cai, F. Lewis, G. Hu, and J. Huang, "The adaptive distributed observer approach to the cooperative output regulation of linear multi-agent systems," *Automatica*, vol. 75, pp. 299–305, 2017.

[9] W. Han, H. Trentelman, Z. Wang, and Y. Shen, "A simple approach to distributed observer design for linear systems," *IEEE Trans. Autom. Control*, vol. 64, no. 1, pp. 329–336, Jan. 2019.

[10] Y. Hong, G. Chen, and L. Bushnell, "Distributed observers design for leader-following control of multi-agent networks," *Automatica*, vol. 44, no. 3, pp. 846–850, 2008.

[11] H. Zhang, F. Lewis, and A. Das, "Optimal design for synchronization of cooperative systems: State feedback, observer and output feedback," *IEEE Trans. Autom. Control*, vol. 56, no. 8, pp. 1948–1952, Aug. 2011.

[12] A. Mitra and S. Sundaram, "Distributed observers for LTI systems," *IEEE Trans. Autom. Control*, vol. 63, no. 11, pp. 3689–3704, Nov. 2018.

[13] W. Han, H. Trentelman, Z. Wang, and Y. Shen, "Towards a minimal order distributed observer for linear systems," *Syst. Control Lett.*, vol. 114, pp. 59–65, 2018.

[14] T. Kim, C. Lee, and H. Shim, "Completely decentralized design of distributed observer for linear systems," *IEEE Trans. Autom. Control*, vol. 65, no. 11, pp. 4664–4678, Nov. 2020.

[15] L. Gao, Y. Cui, and W. Chen, "Admissible consensus for descriptor multiagent systems via distributed observer-based protocols," *J. Franklin Inst.*, vol. 354, no. 1, pp. 257–276, 2017.

[16] X. Zhang, K. Hengster-Movrić, M. Šebek, W. Desmet, and C. Faria, "Distributed observer and controller design for spatially interconnected systems," *IEEE Trans. Control Syst. Technol.*, vol. 27, no. 1, pp. 1–13, Jan. 2019.

[17] Y. Wan, J. Cao, G. Chen, and W. Huang, "Distributed observer-based cybersecurity control of complex dynamical networks," *IEEE Trans. Circuits Syst. I., Reg. Papers*, vol. 64, no. 11, pp. 2966–2975, Nov. 2017.

[18] T. Liu and J. Huang, "A distributed observer for a class of nonlinear systems and its application to a leader-following consensus problem," *IEEE Trans. Autom. Control*, vol. 64, no. 3, pp. 1221–1227, Mar. 2019.

[19] B. Huang and Z. Meng, "Cooperative output regulation for a group of nonlinear systems with limited information exchange: A distributed observer approach," *Syst. Control Lett.*, vol. 128, pp. 46–55, 2019.

[20] W. Wang and Z. Xiang, "Finite-time consensus of nonlinear multiagent systems with nonidentical input delays via event-triggered observer," *IEEE Syst. J.*, vol. 16, no. 4, pp. 5962–5972, 2022.

[21] F. Mazenc and O. Bernard, "Interval observers for linear time-invariant systems with disturbances," *Automatica*, vol. 47, no. 1, pp. 140–147, 2011.

[22] T. Raïssi, D. Efimov, and A. Zolghadri, "Interval state estimation for a class of nonlinear systems," *IEEE Trans. Autom. Control*, vol. 57, no. 1, pp. 260–265, Jan. 2012.

[23] D. Efimov, L. Fridman, T. Raïssi, A. Zolghadri, and R. Seydou, "Interval estimation for LPV systems applying high order sliding mode techniques," *Automatica*, vol. 48, no. 9, pp. 2365–2371, 2012.

[24] R. Thabet, T. Raissi, C. Combastel, D. Efimov, and A. Zolghadri, "An effective method to interval observer design for time-varying systems," *Automatica*, vol. 50, no. 10, pp. 2677–2684, 2014.

[25] H. Ethabet, D. Rabehi, D. Efimov, and T. Raïssi, "Interval estimation for continuous-time switched linear systems," *Automatica*, vol. 90, pp. 230–238, 2018.

[26] T. Alamo, J. Bravo, and E. Camacho, "Guaranteed state estimation by zonotopes," *Automatica*, vol. 41, no. 6, pp. 1035–1043, 2005.

[27] W. Tang, Z. Wang, Y. Wang, T. Raïssi, and Y. Shen, "Interval estimation methods for discrete-time linear time-invariant systems," *IEEE Trans. Autom. Control*, vol. 64, no. 11, pp. 4717–4724, Nov. 2019.

[28] J. Huang, X. Ma, H. Che, and Z. Han, "Further result on interval observer design for discrete-time switched systems and application to circuit systems," *IEEE Trans. Circuits Syst. II- Exp. Briefs*, vol. 67, no. 11, pp. 2542–2546, Nov. 2020.

[29] J. Huang, H. Che, T. Raïssi, and Z. Wang, "Functional interval observer for discrete-time switched descriptor systems," *IEEE Trans. Autom. Control*, vol. 67, no. 5, pp. 2497–2504, May 2022.

[30] H. Zhang, J. Huang, H. Che, and Z. Han, "Optimal interval observer for discrete-time switched systems," *IEEE Trans. Circuits Syst. II- Exp. Briefs*, vol. 69, no. 3, pp. 1233–1237, Mar. 2022.

[31] Z. Zhang and G. Yang, "Distributed fault detection and isolation for multiagent systems: An interval observer approach," *IEEE Trans. Syst. Man Cybern. Syst.*, vol. 50, no. 6, pp. 2220–2230, Jun. 2020.

[32] X. Wang, X. Wang, H. Su, and J. Lam, "Coordination control for uncertain networked systems using interval observers," *IEEE Trans. Cybern.*, vol. 50, no. 9, pp. 4008–4019, Sep. 2020.

[33] X. Luo, X. Wang, M. Zhang, and X. Guan, "Distributed detection and isolation of bias injection attack in smart energy grid via interval observer," *Appl. Energy*, vol. 256, 2019, Art. no. 113703.

[34] X. Wang, X. Luo, M. Zhang, Z. Jiang, and X. Guan, "Detection and localization of biased load attacks in smart grids via interval observer," *Inf. Sci.*, vol. 552, pp. 291–309, 2021.

[35] D. Huong, H. Trinh, and H. Trinh, "Distributed functional interval observers for nonlinear interconnected systems with time-delays and additive disturbances," *IEEE Syst. J.*, vol. 15, no. 1, pp. 411–422, Mar. 2021.

[36] T. Dinh, G. Marouani, T. Raïssi, Z. Wang, and H. Messaoud, "Optimal interval observers for discrete-time linear switched systems," *Int. J. Control*, vol. 93, no. 11, pp. 2613–2621, 2020.

[37] F. Xu, S. Yang, and X. Wang, "A novel set-theoretic interval observer for discrete linear time-invariant systems," *IEEE Trans. Autom. Control*, vol. 66, no. 2, pp. 773–780, Feb. 2021.

[38] H. Song, D. Ding, H. Dong, and X. Yi, "Distributed filtering based on cauchy-kernel-based maximum correntropy subject to randomly occurring cyber-attacks," *Automatica*, vol. 135, 2022, Art. no. 110004.

[39] A. Khan, W. Xie, L. Zhang, and L. Liu, "Design and applications of interval observers for uncertain dynamical systems," *IET Circuit Device Syst.*, vol. 14, no. 6, pp. 721–740, 2020.

[40] A. Khan, W. Xie, B. Zhang, and L. Liu, "A survey of interval observers design methods and implementation for uncertain systems," *J. Franklin Inst.*, vol. 358, no. 6, pp. 3077–3126, 2021.

[41] Y. Ju, X. Tian, H. Liu, and L. Ma, "Fault detection of networked dynamical systems: A survey of trends and techniques," *Int. J. Syst. Sci.*, vol. 52, no. 16, pp. 3390–3409, 2021.

[42] W. Yu, G. Chen, M. Cao, and J. Kurths, "Second-order consensus for multiagent systems with directed topologies and nonlinear dynamics," *IEEE Trans. Syst., Man, Cybern., Syst.*, vol. 40, no. 3, pp. 881–891, Jun. 2010.

[43] Z. Li, X. Liu, M. Fu, and L. Xie, "Global $H_\infty$ consensus of multi-agent systems with Lipschitz non-linear dynamics," *IET Control Theory Appl.*, vol. 6, no. 13, pp. 2041–2048, 2012.

[44] S. Sayyaddelshad and T. Gustafsson, "$H_\infty$ observer design for uncertain nonlinear discrete-time systems with time-delay: LMI optimization approach," *Int. J. Robust Nonlinear Control*, vol. 25, no. 10, pp. 1514–1527, 2015.

[45] C. Combastel, "Zonotopes and kalman observers: Gain optimality under distinct uncertainty paradigms and robust convergence," *Automatica*, vol. 55, pp. 265–273, 2015.

[46] X. Wang, H. Su, F. Zhang, A. Zemouche, and G. Chen, "Interval observer design and consensus of multiagent systems with time-varying interval uncertainties," *SIAM J. Control Optim.*, vol. 59, no. 5, pp. 3392–3417, 2021.

[47] H. Smith, *Monotone Dynamical Systems: An Introduction to the Theory of Competitive and Cooperative Systems*. Providence, RI, USA: Amer. Math. Soc., 1995.

[48] W. Tang, Z. Wang, and Y. Shen, "Interval estimation for discrete-time linear systems: A two-step method," *Syst. Control Lett.*, vol. 123, pp. 69–74, 2019.

[49] X. Li, G. Wei, and D. Ding, "Distributed resilient interval estimation for sensor networks under aperiodic denial-of-service attacks and adaptive event-triggered protocols," *Appl. Math. Comput.*, vol. 409, 2021, Art. no. 126371.